Journal of Magnetic Resonance **139,** 152–164 (1999)
Article ID jmre.1999.1771, available online at http://www.idealibrary.com on IDEAL®

Berry's Phase in the Presence of a Non-adiabatic Environment with an Application to Magnetic Resonance

Frank Gaitan

Department of Physics, Boston College, Chestnut Hill, Massachusetts 02167-3811

Received December 18, 1998; revised March 22, 1999

We consider a two-level system coupled to an environment that evolves non-adiabatically. We present a non-perturbative method for determining the persistence amplitude whose phase contains all the corrections to Berry's phase produced by the non-adiabatic motion of the environment. Specifically, it includes the effect of transitions between the two energy levels to all orders in the non-adiabatic coupling. The problem of determining all non-adiabatic corrections is reduced to solving an ordinary differential equation to which numerical methods should provide solutions in a variety of situations. We apply our method to a particular example that can be realized as a magnetic resonance experiment, thus raising the possibility of testing our results in the laboratory.

I. INTRODUCTION

In the original Berry phase scenario (*1*), the focus of attention is a quantum system with a discrete, non-degenerate energy spectrum. Its Hamiltonian $H[\mathbf{R}]$ is assumed to depend on a set of classical parameters $\mathbf{R}$ which represents an environmental degree of freedom to which the quantum system is coupled. The environment is assumed to evolve adiabatically. This produces an adiabatic time dependence in the quantum Hamiltonian, $H = H[\mathbf{R}(t)]$. The time dependence of the quantum state $|\psi(t)\rangle$ is determined by solving Schrödinger's equation using the quantum adiabatic theorem. Toward this end, one introduces the energy eigenstates of the instantaneous Hamiltonian $H[\mathbf{R}(t)]$,

$$H[\mathbf{R}(t)]|E[\mathbf{R}(t)]\rangle = E[\mathbf{R}(t)]|E[\mathbf{R}(t)]\rangle,$$

and the quantum system is assumed to be initially prepared in an eigenstate $|E[\mathbf{R}(0)]\rangle$ of the initial Hamiltonian $H[\mathbf{R}(0)]$. The quantum adiabatic theorem states that, at time t, the quantum system will be found in the state $|E[\mathbf{R}(t)]\rangle$ to within a phase factor,

$$|\psi(t)\rangle = \exp\left[i\gamma_E(t) - \frac{i}{\hbar}\int_0^t d\tau E[\mathbf{R}(\tau)] \right] |E[\mathbf{R}(t)]\rangle. \quad [1]$$

The second term in the phase of the exponential is known as the dynamical phase and was already familiar from previous studies of the quantum adiabatic theorem. The first term represents Berry's discovery, and is referred to as Berry's phase,

$$\gamma_E(t) = i\int_0^t d\tau \left\langle E[\mathbf{R}(\tau)] \left| \frac{\partial}{\partial \tau} \right| E[\mathbf{R}(\tau)] \right\rangle. \quad [2]$$

In the cases where Berry's phase is physically relevant, γ_E is non-integrable: it cannot be written as a single-valued function of $\mathbf{R}$ over all of parameter space. Simon (*2*) showed that the quantum adiabatic theorem has a line bundle structure inherent in it, and that Schrödinger's equation defines a parallel transport of the quantum state around the line bundle. Berry's phase is the signature that the associated connection has non-vanishing curvature. In this paper we will consider Berry's original scenario for a two-level system (2LS), though we will remove the adiabatic restriction on the environment. Our goal is to obtain the corrections to Berry's phase produced by non-adiabatic effects.

The organization of this paper is as follows. In Section II, we introduce a non-perturbative method for determining all non-adiabatic corrections to Berry's phase. From the derivation, it will be clear that the effect of transitions between the two energy levels has been included to all orders in the non-adiabatic coupling. The problem of determining these corrections is reduced to solving an ordinary differential equation, to which numerical methods should provide solutions in a variety of situations. In Section III we work out a particular example in great detail. In Section IIIA we apply our method to this example and determine exactly the non-adiabatic corrections to Berry's phase. As a test of our method, in Section IIIB we solve the Schrödinger equation exactly, using a rotating frame transformation, and use this solution to independently obtain the non-adiabatic corrections to Berry's phase. Comparison with the result obtained in Section IIIA shows that both methods yield the same result. In Section IIIC we examine the corrections to Berry's phase obtained from our analysis in the limit of weak non-adiabaticity. We carry out this analysis both numerically and analytically. In Section IIID, we discuss a magnetic resonance experiment that provides a realization of

1090-7807/99 $30.00

this particular example, and show how the non-adiabatic corrections to Berry's phase can be observed in measurements of the transverse magnetization. Finally, we make closing remarks in Section IV.

II. GENERAL ANALYSIS

As mentioned in the Introduction, we consider a 2LS coupled to an environmental degree of freedom $\mathbf{R}(t) = R(t)$ (sin θ cos ϕ, sin θ sin ϕ, cos θ) with non-adiabatic time dependence, and for which $R(t) \neq 0$ for all t. The coupling is described by the Hamiltonian,

$$H(t) = \mathbf{R}(t) \cdot \sigma. \tag{3}$$

We denote the instantaneous eigenstates of $H(t)$ by $|E_{\pm}(t)\rangle$ with corresponding eigenvalues $E_{\pm}(t) = \pm R(t)$. Because $R(t) \neq 0$, the energy spectrum is non-degenerate throughout the 2LS's dynamical evolution.

Because $H(t)$ has non-adiabatic time dependence, transitions are possible between the two energy levels. Consequently, if we initially prepare the 2LS in the negative energy level $|E_{-}(0)\rangle$, there is a finite probability amplitude $T_{-}(t)$ to find the 2LS in the positive energy level $|E_{+}(t)\rangle$ at time t. $T_{-}(t)$ is the transition amplitude, and the subscript indicates that the transition began in the negative energy level. Similarly, the probability amplitude that the system is found again in the negative energy level at time t defines the persistence amplitude $P_{-}(t)$. The subscript again indicates that the system was initially in the negative energy level. The amplitudes $P_{+}(t)$ and $T_{+}(t)$ have analogous definitions.

The 2LS dynamics is determined by the propagator $U(t, 0) = \exp[-(i/\hbar) \int_0^t d\tau H(\tau)]$:

$$U(t, 0)|E_{\pm}(0)\rangle = P_{\pm}(t)|E_{\pm}(t)\rangle + T_{\pm}(t)|E_{\mp}(t)\rangle. \tag{4}$$

We will determine $P_{-}(t)$ and $T_{-}(t)$ below, though our principle interest is in $P_{-}(t)$. The following derivation is easily adapted to determine $P_{+}(t)$ and $T_{+}(t)$, though we will not provide that derivation here. It proves convenient to write $U(t, 0)$ as a 2×2 matrix:

$$U(t, 0) = \sum_{E_i(t), E_j(0)} U_{ij}(t)|E_i(t)\rangle\langle E_j(0)| = \begin{pmatrix} P_{+}(t) & T_{-}(t) \\ T_{+}(t) & P_{-}(t) \end{pmatrix}. \tag{5}$$

To begin, we divide the time interval $(0, t)$ into n shorter time intervals of duration $\epsilon = t/n$ by introducing intermediate times $t_k = k\epsilon$ $(k = 0, \cdots, n)$. Later we will let $n \to \infty$. We denote the propagator for the time interval $t_k \to t_{k+1}$ by $U(k) \equiv U(t_{k+1}, t_k)$ so that

$$U(t, 0) = U(n - 1) \cdots U(0). \tag{6}$$

$U(k)$ has the same structure as Eq. [5]:

$$U(k) = \begin{pmatrix} \Delta P_{+}(k) & \Delta T_{-}(k) \\ \Delta T_{+}(k) & \Delta P_{-}(k) \end{pmatrix}. \tag{7}$$

As the notation implies, $\Delta P_{\pm}(k) \equiv \Delta P_{\pm}(t_{k+1}, t_k)$ and $\Delta T_{\pm}(k) \equiv \Delta T_{\pm}(t_{k+1}, t_k)$ are, respectively, the persistence and transition amplitudes corresponding to the time interval $t_k \to t_{k+1}$. Noting that

$$U(k) \approx 1 - \frac{i\epsilon}{\hbar} H(k) + \mathbb{O}(\epsilon^2), \tag{8}$$

$$\langle E_{\pm}(k)| \approx \langle E_{\pm}(k - 1)| + \epsilon \frac{\partial}{\partial t} \langle E_{\pm}(k - 1)| + \mathbb{O}(\epsilon^2), \tag{9}$$

and using Eqs. [5], [8], and [9], one finds that

$$\begin{aligned} \Delta P_{\pm}(k) &= 1 + i\epsilon\dot{\gamma}_{\pm}(k) - \frac{i\epsilon}{\hbar} E_{\pm}(k); \\ \Delta T_{\pm}(k) &= -\epsilon\Gamma_{\pm}(k). \end{aligned} \tag{10}$$

Here a dot over a symbol indicates time differentiation, and

$$\begin{aligned} i\dot{\gamma}_{\pm}(k) &= -\langle E_{\pm}(k)|\dot{E}_{\pm}(k)\rangle; \\ \Gamma_{\pm}(k) &= \langle E_{\mp}(k)|\dot{E}_{\pm}(k)\rangle, \end{aligned} \tag{11}$$

with

$$\Gamma_{+}(k) = -\Gamma^{*}_{-}(k).$$

$\gamma_{\pm}(k)$ are the Berry phases for the $\pm$ energy levels, and normalizability of the instantaneous energy eigenstates insures that the Berry phases are real. $\Gamma_{\pm}(k)$ are known as the non-adiabatic couplings for the $\pm$ energy levels, and generally are complex-valued.

Inserting Eq. [7] repeatedly into Eq. [6], and carrying out the necessary matrix multiplications, one can show using induction that

$$\begin{aligned} P_{-}(t) = &\prod_{k=0}^{n-1} \Delta P_{-}(k) + [\prod_{k=n_1+1}^{n-1} \Delta P_{-}(k)][\Delta T_{+}(n_1)] \\ &\times [\prod_{k=n_2+1}^{n_1-1} \Delta P_{+}(k)][\Delta T_{-}(n_2)] \\ &\times [\prod_{k=0}^{n_2-1} \Delta P_{-}(k)] + \cdots. \end{aligned} \tag{12}$$

We can make this equation more intelligible by introducing the

amplitudes $\mathcal{P}_{\pm}(i, j)$ to persist *without* any transitions in a given energy level over the time interval $t_j \to t_i$:

$$\mathcal{P}_{\pm}(i, j) = \prod_{k=j}^{i-1} \Delta P_{\pm}(k).$$

Note that $\Delta P_{\pm}(i-1)$ is the persistence amplitude corresponding to the time interval $t_{i-1} \to t_i$. This is why the upper limit on the product must be $i-1$, and not i. Equation [12] can then be rewritten as

$$P_{-}(t) = \mathcal{P}_{-}(n, 0) + \mathcal{P}_{-}(n, n_1 + 1)\Delta T_{+}(n_1) \times \mathcal{P}_{+}(n_1, n_2 + 1)\Delta T_{-}(n_2)\mathcal{P}_{-}(n_2, 0) + \cdots . \quad [13]$$

Each term in Eq. [13] gives the amplitude for the state of the 2LS to follow a particular time sequence that begins and ends in the negative energy level. For any given time sequence, each subinterval will have an amplitude associated with it that indicates whether a transition occurred during it ($\Delta T(k)$), or not ($\Delta P(k)$). Thus the first term gives the amplitude for the system to undergo zero transitions; the second term gives the amplitude for two transitions to occur (in subintervals n_1 and n_2). The remaining terms correspond to 4-transitions, 6-transitions, etc. Only an even number of transitions is possible since the time development begins and ends in the negative energy level. Thus each transition out of this level must eventually be followed by a transition back into it. One can set up a diagrammatic calculus to produce all the terms in Eq. [13], complete with rules for assigning a probability amplitude to each diagram, though we will not take the time to work that out here.

Similarly, one can show that

$$T_{-}(t) = \mathcal{P}_{+}(n, n_1 + 1)\Delta T_{-}(n_1)\mathcal{P}_{-}(n_1, 0) + \mathcal{P}_{+}(n, n_1 + 1)\Delta T_{-}(n_1)\mathcal{P}_{-}(n_1, n_2 + 1) \times \Delta T_{+}(n_2)\mathcal{P}_{+}(n_2, n_3 + 1) \times \Delta T_{-}(n_3)\mathcal{P}_{-}(n_3, 0) + \cdots . \quad [14]$$

Here only an odd number of transitions can occur since the 2LS must finish in the positive energy level after having started in the negative energy level. Further simplification is possible if we introduce

$$E(n_1, n_2) = \Delta T_{+}(n_1)\mathcal{P}_{+}(n_1, n_2 + 1) \times \mathcal{P}_{-}^{-1}(n_1, n_2 + 1)\Delta T_{-}(n_2),$$

and insert $1 = \mathcal{P}_{-}(k)\mathcal{P}_{-}^{-1}(k)$ appropriately into Eqs. [13] and [14]. One finds that

$$P_{-}(t) = \mathcal{P}_{-}(n, 0)[1 + E(n_1, n_2) + E(n_1, n_2)E(n_3, n_4) + \cdots],$$

and

$$T_{-}(t) = \mathcal{P}_{-}(n, 0)\{\mathcal{P}_{+}(n, n_1 + 1)\Delta T_{-}(n_1)\mathcal{P}_{-}^{-1}(n, n_1 + 1)\} \times [1 + E(n_2, n_3) + E(n_2, n_3)E(n_4, n_5) + \cdots].$$

Using Eq. [10], and recalling that n is large, one can show that

$$\mathcal{P}_{\pm}(n_1, n_2) = \exp[\sum_{k=n_2}^{n_1-1} \epsilon\{i\dot{\gamma}_{\pm}(k) - (i/\hbar)E_{\pm}(k)\}],$$

and

$$E(n_1, n_2) = -[\epsilon F^*(n_1 - 1)][\epsilon F(n_2 + 1)],$$

with

$$F(m) = \Gamma_{-}(m)\exp\left[\frac{i}{\hbar}\sum_{k=0}^{m} \epsilon\{(E_{+}(k) - E_{-}(k)) - \hbar(\dot{\gamma}_{+}(k) - \dot{\gamma}_{-}(k))\}\right].$$

So far, we have only considered one particular choice of intermediate times. We must now sum over all t_k (maintaining the proper time orderings). This yields the following expression for $P_{-}(t)$,

$$P_{-}(t) = \exp\left[i\gamma_{-}(t) - \frac{i}{\hbar}\int_0^t d\tau E_{-}(\tau)\right]S(t), \quad [15]$$

where

$$S(t) = 1 - \int_0^t dy_1 F^*(y_1)\int_0^{y_1} dx_1 F(x_1) + \int_0^t dy_1 F^*(y_1)\int_0^{y_1} dx_1 F(x_1) \times \int_0^{x_1} dy_2 F^*(y_2)\int_0^{y_2} dx_2 F(x_2) - \cdots , \quad [16]$$

and

$$F(t) = \Gamma_-(t)\exp\left[i \int_0^t d\tau\delta(\tau) \right];$$

$$\delta(\tau) = \left[\frac{E_+(\tau) - E_-(\tau)}{\hbar} - (\dot{\gamma}_+(\tau) - \dot{\gamma}_-(\tau)) \right]. \qquad [17]$$

We see that $S(t) = A(t)\exp[i\rho(t)]$ contains all the consequences of the non-adiabatic time dependence, and that it includes transitions between the levels to all orders in the non-adiabatic couplings $\Gamma_\pm(t)$. It is also clear that $\rho(t)$ contains all the non-adiabatic corrections to Berry's phase $\gamma_-(t)$. We close this section by presenting a procedure for evaluating $S(t)$ which promises to be useful in a variety of situations.

It is a simple matter to write Eq. [16] as an integral equation for $S(t)$:

$$S(t) = 1 - \int_0^t dy F^*(y) \int_0^y dx F(x) S(x). \qquad [18]$$

Introducing the auxiliary quantity $I(t)$,

$$I(t) = \int_0^t dx F(x) S(x) \Leftrightarrow S(t) = \frac{1}{F(t)} \frac{dI}{dt}, \qquad [19]$$

and differentiating Eq. [18] with respect to t yield an ordinary differential equation for $I(t)$:

$$\frac{d^2I}{dt^2} + \left(\frac{\dot{F}}{F} \right) \frac{dI}{dt} + |F|^2 I = 0. \qquad [20]$$

From Eq. [19], the appropriate initial conditions are $I(0) = 0$, and $\dot{I}(0) = F(0)$ (note that $S(0) = 1$ according to Eq. [18]). Determining $I(t)$ reduces to solving Eq. [20], either numerically or analytically, which should be possible in a wide variety of circumstances. From $I(t)$ we determine $S(t)$ via Eq. [19], and from $S(t)$ we determine $\rho(t)$ and $A(t)$:

$$\tan \rho(t) = \frac{\text{Im } S(t)}{\text{Re } S(t)};$$

$$A(t) = \sqrt{(\text{Re } S(t))^2 + (\text{Im } S(t))^2}. \qquad [21]$$

$I(t)$ also allows us to express $T_-(t)$ more succinctly. Using the above results, one can show that

$$T_-(t) = -\exp\left[i\gamma_+(t) - \frac{i}{\hbar} \int_0^t d\tau E_+(\tau) \right] I(t). \qquad [22]$$

Equations [15]–[22] constitute a general approach for determining completely the consequences of the non-adiabatic motion of the environment. Specifically, $\rho(t)$ contains all non-adiabatic corrections to Berry's phase, while $A(t)$ describes the reduced amplitude for the 2LS to be found in the negative energy level at time t due to transitions. In the following section, we examine a particular example which is experimentally realizable and yet simple enough that our equations can be evaluated without approximation and tested against the exact solution of the Schrödinger equation.

III. APPLICATION OF GENERAL ANALYSIS TO A PARTICULAR EXAMPLE

In this section we will examine the interaction of a spin $\frac{1}{2}$ with a time-varying magnetic field $\mathbf{B}(t)$. The magnetic field is assumed to precess about the z-axis at a fixed angle θ, at a constant precession rate $\dot{\phi}(t) = \omega$, and with constant magnitude $|\mathbf{B}(t)| = B$. Such magnetic fields are used regularly in experiments involving nuclear magnetic resonance (NMR), so that an experimental test of the results of this section should be possible. The coupling of a spin to a magnetic field is described by the Zeeman Hamiltonian which, for a spin $\frac{1}{2}$, has the same form as Eq. [3] with the substitution $\mathbf{R}(t) = -\gamma\hbar\mathbf{B}(t)/2$. Throughout this section we will stick with the notation of Eq. [3], though it is a simple matter to substitute for $\mathbf{R}(t)$ when necessary. We will occasionally refer to $\mathbf{R}(t)$ as the magnetic field, though this is not literally true.

A. Non-adiabatic Effects: General Analysis

In this subsection, we will determine all non-adiabatic corrections by evaluating $S(t)$ using the general analysis of Section II. To begin, we must determine the instantaneous eigenstates $|E_\pm(t)\rangle$ of $H(t)$. Straightforward analysis of Eq. (3) gives

$$|E_+(t)\rangle = \begin{pmatrix} \cos\theta/2 \\ \sin\theta/2 \exp[i\omega t] \end{pmatrix};$$

$$|E_-(t)\rangle = \begin{pmatrix} \sin\theta/2 \\ -\cos\theta/2 \exp[i\omega t] \end{pmatrix}, \qquad [23]$$

where $\mathbf{R}(t) = R(\sin\theta\cos\omega t, \sin\theta\sin\omega t, \cos\theta)$. Combining Eq. [23] with Eq. [11] gives

$$\begin{cases} \Gamma_-(t) = -i\omega/2 \sin\theta \equiv -iC \\ \delta = 2R/\hbar - \omega\cos\theta \end{cases} \Rightarrow F(t) = -iC \exp[i\delta t]. \qquad [24]$$

$F(t)$ is now inserted into Eq. [20] to give

$$\ddot{I} - i\delta\dot{I} + C^2 I = 0.$$

This equation has constant coefficients and so is easily solved. One finds

$$I(t) = -\frac{i\omega \sin\theta}{\Omega_0} \exp\left[\frac{i\delta t}{2}\right] \sin\left(\frac{\Omega_0 t}{2}\right), \qquad [25]$$

with $\Omega_0 = \sqrt{\delta^2 + 4C^2}$. $S(t)$ follows from Eq. [19]:

$$\text{Re } S(t) = \cos\frac{\delta t}{2}\cos\frac{\Omega_0 t}{2} + \cos\Delta\theta \sin\frac{\delta t}{2}\sin\frac{\Omega_0 t}{2} \qquad [26]$$

$$\text{Im } S(t) = -\sin\frac{\delta t}{2}\cos\frac{\Omega_0 t}{2} + \cos\Delta\theta \cos\frac{\delta t}{2}\sin\frac{\Omega_0 t}{2}. \qquad [27]$$

Here $\cos\Delta\theta = \delta/\Omega_0$: the physical significance of $\Delta\theta$ will become clear in the following subsection.

B. Non-adiabatic Effects: Rotating Frame Analysis

In this subsection we obtain the exact solution to Schrödinger's equation for the particular example considered in this section, and derive from it $S(t)$. This result will be compared with that obtained in Section IIIA, and will thus provide the first test of our approach.

The exact solution can be found using a rotating coordinate frame analysis. In the laboratory frame, the Schrödinger equation is

$$i\hbar\frac{\partial}{\partial t}|\psi(t)\rangle = H(t)|\psi(t)\rangle, \qquad [28]$$

where $H(t)$ is given by Eq. [3]. We can transform to a frame that rotates with $\mathbf{R}(t)$ using the unitary operator

$$\mathcal{U}(t) = \exp\left[-\frac{i\omega t}{2}\sigma_z\right].$$

Writing $|\psi(t)\rangle = \mathcal{U}(t)|\bar{\psi}(t)\rangle$, and substituting into Eq. [28] give the Schrödinger equation in the rotating frame,

$$i\hbar\frac{\partial}{\partial t}|\bar{\psi}(t)\rangle = \bar{H}|\bar{\psi}(t)\rangle,$$

where

$$\bar{H} = \mathcal{U}^\dagger H \mathcal{U} - i\hbar\mathcal{U}^\dagger\dot{\mathcal{U}} = \begin{pmatrix} \{R\cos\theta - \hbar\omega/2\} & R\sin\theta \\ R\sin\theta & -\{R\cos\theta - \hbar\omega/2\} \end{pmatrix}.$$

$\bar{H}$ is clearly time-independent, as expected, since the magnetic field is stationary in the rotating frame. The z-component of the magnetic field has been altered by the transformation. The magnetic field now makes an angle $\bar{\theta}$ with the z-axis given by

$$\tan\bar{\theta} = \frac{R\sin\theta}{R\cos\theta - \hbar\omega/2}. \qquad [29]$$

Note that $\bar{\phi} = 0$ since $\bar{H}$ is real.

Because it is time-independent, $\bar{H}$ has stationary states. The energies are

$$\bar{E}_\pm = \pm\sqrt{\left(R\cos\theta - \frac{\hbar\omega}{2}\right)^2 + R^2\sin^2\theta} = \pm\frac{\hbar\Omega_0}{2}, \qquad [30]$$

and Ω_0 was defined in Sec. IIIA. The eigenstates are

$$|\bar{E}_+\rangle = \begin{pmatrix} \cos\bar{\theta}/2 \\ \sin\bar{\theta}/2 \end{pmatrix}; \quad |\bar{E}_-\rangle = \begin{pmatrix} \sin\bar{\theta}/2 \\ -\cos\bar{\theta}/2 \end{pmatrix}. \qquad [31]$$

The initial condition in the lab frame is $|\psi(0)\rangle = |E_-(0)\rangle$, and $|E_-(0)\rangle$ is given in Eq. [23]. Since $U(0) = 1$, the initial condition in the rotating frame is $|\bar{\psi}(0)\rangle = |E_-(0)\rangle$. Expanding $|\bar{\psi}(0)\rangle$ in the basis $|\bar{E}_\pm\rangle$ gives

$$|\bar{\psi}(0)\rangle = a_+|\bar{E}_+\rangle + a_-|\bar{E}_-\rangle, \qquad [32]$$

and application of the initial condition gives

$$a_+ = -\sin\frac{\Delta\theta}{2}; \quad a_- = \cos\frac{\Delta\theta}{2}. \qquad [33]$$

Here $\Delta\theta \equiv \bar{\theta} - \theta$, and is the same $\Delta\theta$ that appeared in Section IIIA. One can see this by using Eq. [29] and standard trigonometric identities to show that $\cos\Delta\theta = \delta/\Omega_0$, just as we found for $\Delta\theta$ in Section IIIA. Physically, $\Delta\theta$ is the change in the angle the magnetic field makes with the z-axis, as seen in the rotating and lab frames. From Eq. [32] we can immediately write

$$|\bar{\psi}(t)\rangle = a_+\exp\left[-\frac{i\Omega_0 t}{2}\right]|\bar{E}_+\rangle + a_-\exp\left[\frac{i\Omega_0 t}{2}\right]|\bar{E}_-\rangle.$$

Transforming back to the lab frame gives the exact solution $|\psi(t)\rangle$:

$$|\psi(t)\rangle = \exp\left[-\frac{i\omega t}{2}\right]\left\{a_+\exp\left[-\frac{i\Omega_0 t}{2}\right] \times \begin{pmatrix} \cos\bar{\theta}/2 \\ \sin\bar{\theta}/2\,\exp[i\omega t] \end{pmatrix} + a_-\exp\left[\frac{i\Omega_0 t}{2}\right] \times \begin{pmatrix} \sin\bar{\theta}/2 \\ -\cos\bar{\theta}/2\,\exp[i\omega t] \end{pmatrix}\right\}. \qquad [34]$$

From Eq. [34] we can obtain the persistence amplitude $P_-(t) = \langle E_-(t)|\psi(t)\rangle$. Using Eq. [23], we find

$$P_-(t) = \exp\left[-\frac{i\omega t}{2}\right]\left\{a_+^2\exp\left[-\frac{i\Omega_0 t}{2}\right] + a_-^2\exp\left[\frac{i\Omega_0 t}{2}\right]\right\}.$$

This expression can be rewritten straightforwardly as

$$P_-(t) = \exp\left[i\gamma_- - \frac{i}{\hbar}\int_0^t d\tau E_-(\tau)\right] \times\left\{\exp\left[-\frac{i\delta t}{2}\right]\left(a_+^2\exp\left[-\frac{i\Omega_0 t}{2}\right] + a_-^2\exp\left[\frac{i\Omega_0 t}{2}\right]\right)\right\}.$$

Thus, the factor in curly brackets is $S(t)$ (see Eq. [15]), as determined from the exact solution of Schrödinger's equation. The exact solution thus yields

$$\text{Re } S(t) = \cos\frac{\delta t}{2}\cos\frac{\Omega_0 t}{2} + \cos\Delta\theta\sin\frac{\delta t}{2}\sin\frac{\Omega_0 t}{2} \quad [35]$$

$$\text{Im } S(t) = -\sin\frac{\delta t}{2}\cos\frac{\Omega_0 t}{2} + \cos\Delta\theta\cos\frac{\delta t}{2}\sin\frac{\Omega_0 t}{2}. \quad [36]$$

Comparing Eqs. [35] and [36] with Eqs. [26] and [27], we see that our approach gives precisely the same result for $S(t)$ as the exact solution of the Schrödinger equation.

C. Non-adiabatic Effects: Numerical and Analytical Evaluation

Here we explicitly evaluate the non-adiabatic corrections to Berry's phase. The exact result ρ containing all non-adiabatic corrections will be evaluated numerically, while an approximate analysis will be used to determine these corrections analytically in the limit of weak non-adiabaticity. We also compare our results with two previous calculations of ρ in the literature.

We begin our analysis by substituting Eqs. [26] and [27] into Eq. [21] to determine ρ. This yields

$$\tan\rho = \frac{[g\tan\Omega_0 t/2] - \tan\delta t/2}{1 + [g\tan\Omega_0 t/2]\tan\delta t/2}, \quad [37]$$

where $g \equiv \cos\Delta\theta = \delta/\Omega_0$. With ε introduced through the relation

$$\tan\frac{\varepsilon t}{2} = g\tan\frac{\Omega_0 t}{2}, \quad [38]$$

Eq. [37] becomes

$$\tan\rho = \tan\left[\frac{(\varepsilon-\delta)t}{2}\right],$$

so that

$$\rho = \frac{(\varepsilon-\delta)}{2}t. \quad [39]$$

Clearly, we must determine ε. To this end, we introduce the definitions

$$x = \frac{\hbar\omega}{2R}; \quad s = \left(\frac{\omega}{2\pi}\right)t; \quad \epsilon = \left(\frac{\hbar}{2R}\right)\varepsilon; \quad [40]$$

as well as dimensionless versions of δ and Ω_0 (see Section IIIA):

$$d = \left(\frac{\hbar}{2R}\right)\delta = 1 - x\cos\theta \quad [41]$$

$$e = \left(\frac{\hbar}{2R}\right)\Omega_0 = \sqrt{1 - 2x\cos\theta + x^2}. \quad [42]$$

Finally, from its definition below Eq. [37], we have

$$g = \frac{1 - x\cos\theta}{\sqrt{1 - 2x\cos\theta + x^2}} = 1 - \frac{x^2}{2}\sin^2\theta - x^3\sin^2\theta\cos\theta + \mathcal{O}(x^4). \quad [43]$$

In terms of these dimensionless quantities, Eq. [38] becomes

$$\tan\left(\frac{\pi s}{x}\epsilon\right) = g\tan\left(\frac{\pi s}{x}e\right). \quad [44]$$

It is a straightforward matter to numerically invert Eq. [44] to obtain ϵ, and then, from Eqs. [40] and [39], to determine ρ exactly. Before presenting our numerical results, we will determine ϵ analytically, in the limit of weak non-adiabaticity ($x \ll 1$). This will give an approximate analytical result for ρ which can then be compared with previous work in the literature, as well as with our numerical result.

The starting point for the approximate treatment is the observation that $g = 1 + \delta g$. We will determine ρ to zeroth- and first-order in δg. The zeroth-order result ρ_0 will be found to be identical with an earlier result of Berry (*3*), and of Datta *et al.* (*4*). The first-order result ρ_1 will be found to contain an oscillatory contribution that does not appear in ρ_0. One could go on to work out ρ_n for $n \geq 2$, though we will not do so here.

ϵ is determined to zeroth-order in δg by setting $g \equiv 1$ in Eq. [44]. The zeroth-order (in δg) approximation ϵ_0 thus satisfies

$$\tan\left(\frac{\pi s}{x}\,\epsilon_0\right) = \tan\left(\frac{\pi s}{x}\,e\right),$$

so that

$$\epsilon_0 = e.$$

Using ϵ_0 in Eqs. [40] and [39] gives ρ_0:

$$\rho_0 = \left(\frac{\Omega_0 - \delta}{2}\right) t. \qquad [45]$$

Using Eq. [42], Ω_0 can be expanded to $\mathbb{O}(x^2)$, so that for $x \ll 1$,

$$\rho_0 = \omega t\left[\frac{x}{4}\sin^2\theta + \frac{x^2}{4}\sin^2\theta\cos\theta + \mathbb{O}(x^3)\right]. \qquad [46]$$

Our result for ρ_0 is identical to the weakly non-adiabatic results of Refs. (*3, 4*).

To determine corrections to $\epsilon_0 = e$, we introduce $\Delta\epsilon$ through the relation

$$\epsilon \equiv e + \Delta\epsilon. \qquad [47]$$

Equation [44] becomes

$$\tan\left[\frac{\pi s}{x}\,(e + \Delta\epsilon)\right] = (1 + \delta g)\tan\left(\frac{\pi s}{x}\,e\right).$$

Using the angle-sum formula for the tangent on the LHS, this equation can be rewritten as

$$\tan\left(\frac{\pi s}{x}\,\Delta\epsilon\right) = \frac{1}{2}\sin\left(\frac{2\pi s}{x}\,e\right)\frac{\delta g}{1 + \delta g\,\sin^2((\pi s/x)\,e)}. \qquad [48]$$

Up to this point, Eq. [48] is still exact. From Eq. [43], we see that when $x \ll 1$, $\delta g \ll 1$, so that the first-order (in δg) result $\Delta\epsilon_1$ satisfies

$$\tan\left(\frac{\pi s}{x}\,\Delta\epsilon_1\right) = \frac{1}{2}\sin\left(\frac{2\pi s}{x}\,e\right)\delta g + \mathbb{O}(\delta g^2). \qquad [49]$$

Thus when $x \ll 1$, the RHS of Eq. [49] is small, so that the tangent function on the LHS is well-approximated by its argument

$$\Delta\epsilon_1 = \frac{x}{2\pi s}\sin\left(\frac{2\pi s}{x}\,e\right)\delta g + \mathbb{O}(\delta g^2). \qquad [50]$$

Using Eqs. [50], [47], [40], and [39], we find that

$$\rho_1 = \rho_0 + a(x)\sin\Omega_0 t, \qquad [51]$$

where

$$a(x) = -\frac{1}{2}\left[\frac{x^2}{2}\sin^2\theta + x^3\sin^2\theta\cos\theta\right]. \qquad [52]$$

We see that ρ_1 is qualitatively different from ρ_0 in that it includes a sinusoidally oscillating contribution not present in ρ_0. For $x \ll 1$, the amplitude $a(x) \ll 1$, although it increases with increasing x. Using Eqs. [40] and [42], it follows that

$$\Omega_0 t = \left(\frac{2\pi}{x}\right) s + \mathbb{O}(1), \qquad [53]$$

so that the dimensionless frequency of the sinusoidal oscillation is $2\pi/x$. This frequency is very large when $x \ll 1$, and decreases with increasing x. In the numerical evaluation of ρ, we will set $s = 1$ corresponding to $t = 2\pi/\omega$. In this case, the oscillation has the form $a(x)\sin(2\pi/x)$, so that the number of oscillations swept out in a fixed interval Δx about x decreases as the value of x is increased. We now compare ρ_0 and ρ_1 with the exact numerical result ρ.

In carrying out the numerical calculation, we have set $s = 1$ and $\theta = 60°$. In Fig. 1a we plot ρ and ρ_0 for $0 \le x \le 0.05$. The oscillating curve is the exact result ρ which was determined numerically, while the other curve is ρ_0. It is clear that, for this range of x, we are only seeing the term in ρ_0 that is linear in x (see Eq. [46]). The oscillations expected in ρ from our approximate analysis are clearly visible. The oscillation amplitude increases with increasing x, and the rate of oscillation decreases with increasing x, as expected. In Fig. 1b we plot both ρ/ρ_0 and ρ/ρ_1. The rapidly oscillating curve is ρ/ρ_0. One again sees that the oscillation amplitude increases with increasing x. It is important to note, however, the scale of the vertical axis in this figure, which has been chosen to fully utilize the graphing space. In spite of appearances, the oscillation amplitude is never larger than 0.8% of ρ_0 for the range of x-values considered, so that the oscillations really are of small amplitude. The decrease in the rate of oscillation with increasing x is also clearly apparent. The horizontal line at $R = 1$ in Fig. 1b is ρ/ρ_1. Clearly, the oscillation in ρ_1 gives an excellent account of the oscillations in ρ for the range of x-values considered in this figure. It is because ρ_1 agrees so well with ρ that we did not plot it in Fig. 1a: the two curves overlap so completely that only one curve is seen.

In Fig. 2a we plot ρ and ρ_0 over the range $0 \le x \le 0.1$. The

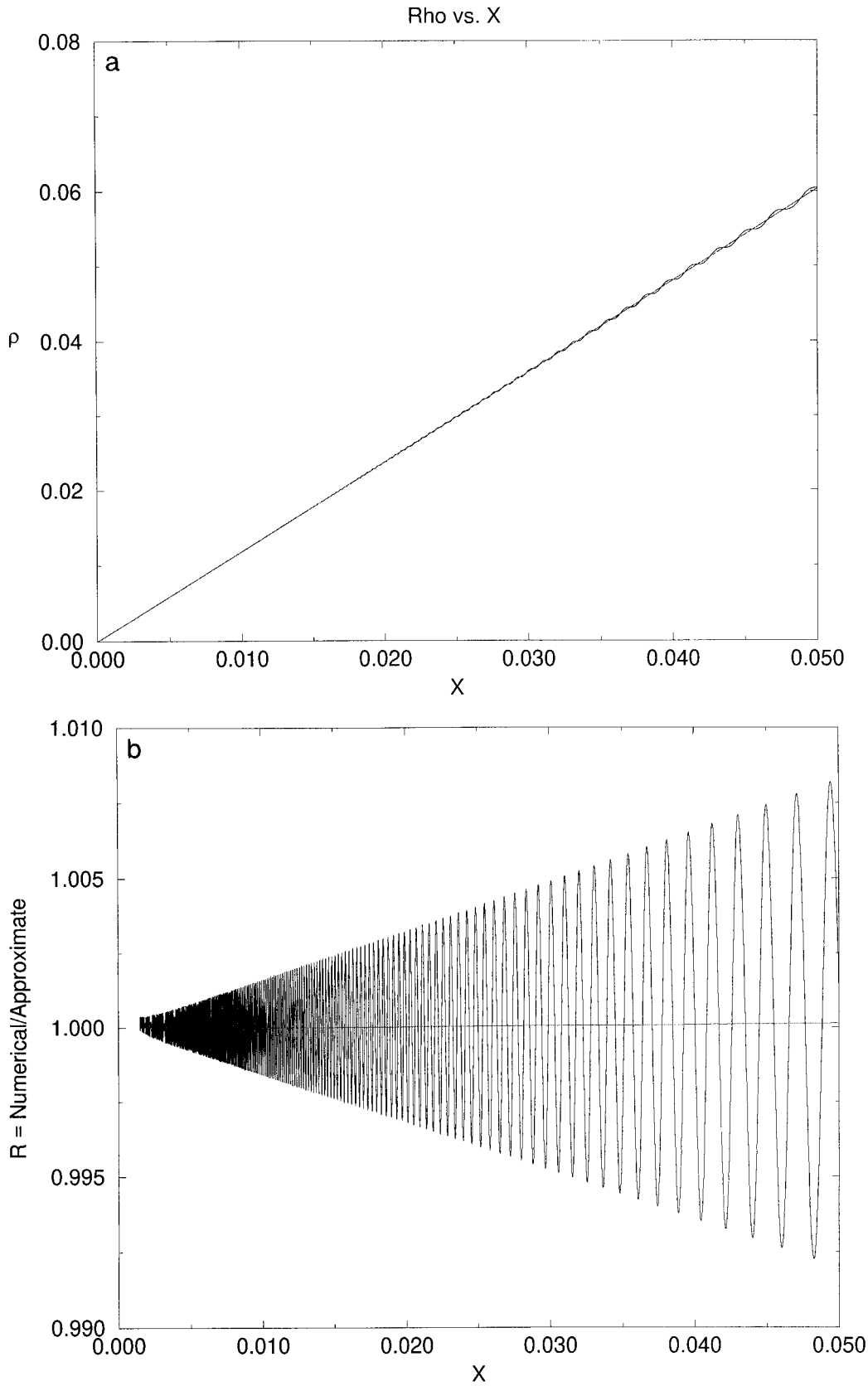

FIG. 1. (a) Plot of non-adiabatic corrections to Berry's phase ρ as a function of $x = \hbar\omega/2R$. The oscillating curve is the numerically determined exact result ρ. The curve that threads the numerical result is the zeroth-order analytical approximation ρ_0. (b) Comparison of the exact numerical result for the non-adiabatic corrections to Berry's phase ρ to the zeroth-order and first-order analytical approximations ρ_0 and ρ_1, respectively. The oscillating curve is the ratio ρ/ρ_0, while the horizontal curve at $R = 1$ is a plot of ρ/ρ_1. Here $x = \hbar\omega/2R$.

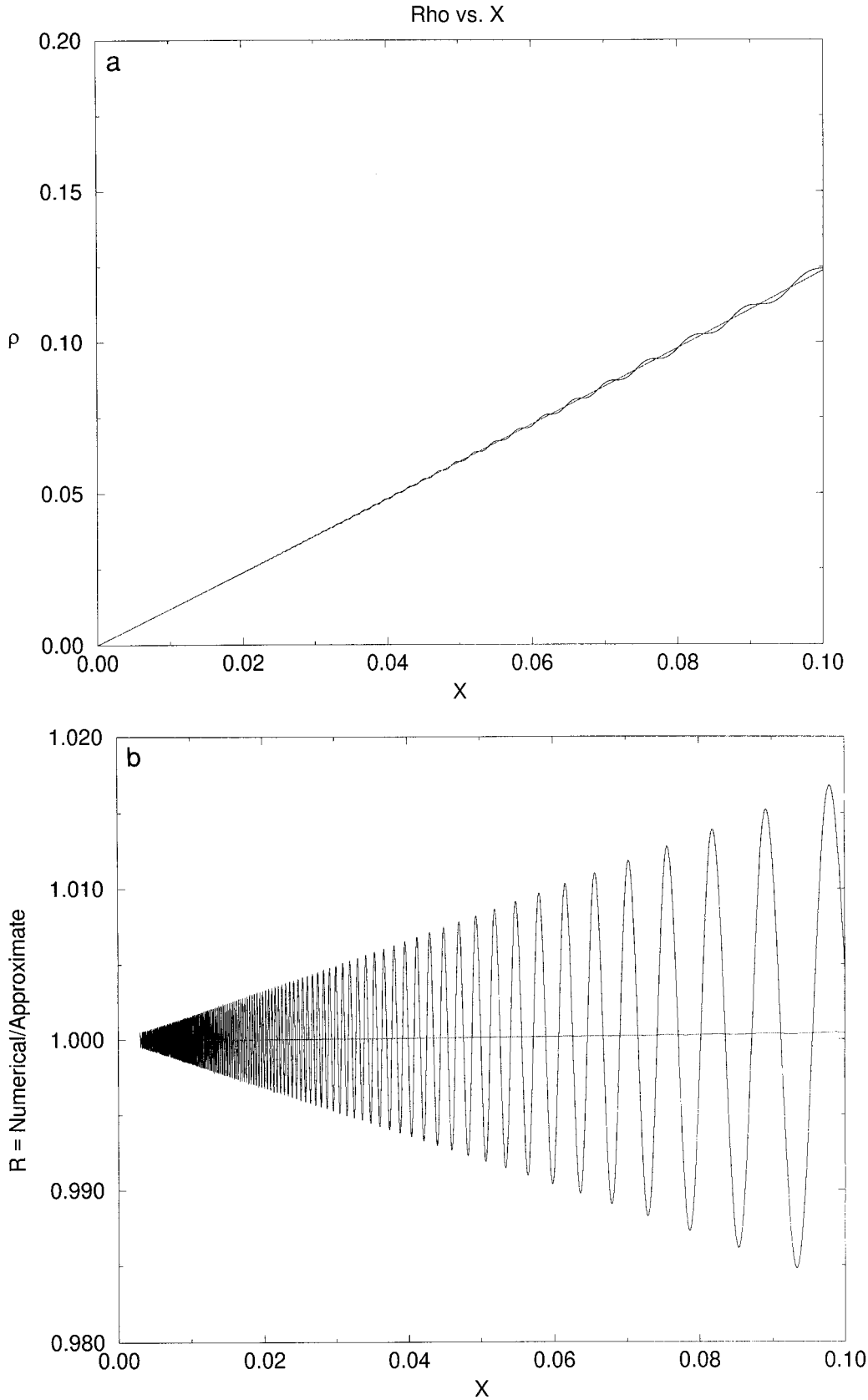

FIG. 2. (a) Plot of the non-adiabatic corrections to Berry's phase ρ as a function of $x = \hbar\omega/2R$. The oscillating curve is the numerically determined exact result ρ. The curve that threads the numerical result is the zeroth-order analytical approximation ρ_0. (b) Comparison of the exact numerical result for the non-adiabatic corrections to Berry's phase ρ to the zeroth-order and first-order analytical approximations ρ_0 and ρ_1, respectively. The oscillating curve is the ratio ρ/ρ_0, while the horizontal curve at $R = 1$ is a plot of ρ/ρ_1. Here $x = \hbar\omega/2R$.

oscillatory curve is the exact numerical result ρ, while the other curve is ρ_0. This figure is qualitatively similar to Fig. 1a, and one sees that ρ_0 is still behaving linearly in x over this range of x-values. In Fig. 2b we plot ρ/ρ_0 and ρ/ρ_1. The oscillatory curve is ρ/ρ_0, and we again see the increase in oscillation amplitude with increasing x, though the amplitude is never larger than 1.8% of ρ_0 over the range of x considered in the figure. The rate of oscillation continues to decrease with increasing x. The (essentially) horizontal line at $R = 1$ is ρ/ρ_1. We see that ρ_1 continues to provide a very good description of ρ, although a tiny residual oscillation is barely apparent.

In Fig. 3a we plot ρ and ρ_1 for $0 \leq x \leq 0.5$. We do *not* plot ρ_0 in this figure since it looks qualitatively similar to Figs. 1a and 2a. For this range of x-values, we are more interested in comparing ρ and ρ_1. We see that ρ_1 still provides a very good approximation for ρ, although a small deviation is noticeable for $0.4 \leq x \leq 0.5$. In Fig. 3b we plot ρ/ρ_1. The deviation of ρ from ρ_1 is much more apparent here because of the scale of the vertical axis in the figure. We see, however, that ρ_1 never exceeds ρ by more than 0.8% of ρ. One also sees that ρ is developing higher frequency oscillations not described by ρ_1. Even so, these differences are not very large over the range of x-values considered, so that ρ_1 still provides a good analytical approximation for the exact ρ for $x \leq 0.4$–0.5.

In the following subsection we show that these non-adiabatic corrections can be observed using NMR. The oscillations in ρ are seen to cause the NMR signal to become frequency modulated, and we present the experimental consequences of this modulation.

D. Experimental Realization: Nuclear Magnetic Resonance

One of the first observations of Berry's phase was made by Suter *et al.* (*5*) using nuclear magnetic resonance (NMR). In this experiment, the rotating magnetic field precessed about the z-axis in the manner assumed in this section. Measurement of the transverse magnetization $\langle M_\perp(t)\rangle$ allowed observation of Berry's phase. We now show that this same measurement (not so surprisingly) will also reveal the non-adiabatic corrections to Berry's phase determined above. We also show that the oscillations present in these corrections cause $\langle M_\perp(t)\rangle$ to become frequency modulated.

If initially the spin $\frac{1}{2}$ has a component transverse to $\mathbf{B}(0)$, the spin will begin to precess about $\mathbf{B}(0)$. If $\mathbf{B}(t)$ does not evolve too rapidly, the spin precession simply follows $\mathbf{B}(t)$. To simplify the analysis, we assume,

$$|\psi(0)\rangle = \frac{1}{\sqrt{2}}\left[|E_+(0)\rangle + |E_-(0)\rangle\right],$$

corresponding to the spin initially aligned along the x-axis in the lab frame. Using $|\psi(t)\rangle = U(t, 0)|\psi(0)\rangle$, and Eq. [4], we have

$$|\psi(t)\rangle = \frac{1}{\sqrt{2}}\left[\{P_+(t) + T_-(t)\}|E_+(t)\rangle + \{P_-(t) + T_+(t)\}|E_-(t)\rangle\right].$$

The transverse magnetization $\langle M_\perp(t)\rangle = \langle M_x(t) + iM_y(t)\rangle$ is given by

$$\langle M_\perp(t)\rangle = \mathrm{Tr}\ \rho_d(t)\{\gamma\hbar I^+\}. \qquad [54]$$

Here $\rho_d(t) = |\psi(t)\rangle\langle\psi(t)|$ is the density matrix; $I^+ = I_x + iI_y$ is the raising operator for angular momentum; and γ is the gyromagnetic ratio. We assume that $t = 2\pi/\omega$ so that $|E_\pm(2\pi/\omega)\rangle = |E_\pm(0)\rangle$. Also, in the basis $|E_\pm(0)\rangle$, $I^+ = |E_+(0)\rangle\langle E_-(0)|$. Using these results in Eq. [54] one finds

$$\langle M_\perp(2\pi/\omega)\rangle = \frac{\gamma\hbar}{2}(P_- + T_+)(P_+^* + T_-^*) = \frac{\gamma\hbar}{2}[P_-P_+^* + T_+P_+^* + P_-T_-^* + T_+T_-^*]. \qquad [55]$$

We have already evaluated P_-. T_- can be evaluated using Eqs. [25] and [22]. P_+ and T_+ are determined by suitably adapting the analyses for P_- and T_-. One finds

$$P_- = A\ \exp\left[\frac{iRt}{\hbar} - \frac{i\omega t}{2}(1 + \cos\theta) + i\rho\right];$$
$$P_+ = A\ \exp\left[-\frac{iRt}{\hbar} - \frac{i\omega t}{2}(1 - \cos\theta) - i\rho\right] \qquad [56]$$

and

$$T_- = -iC\ \exp\left[-\frac{i\omega t}{2}\right]; \quad T_+ = T_-. \qquad [57]$$

A is determined from Eq. [21], and C from Eq. [24].

Using these results in Eq. [55], one finds

$$\langle M_\perp(t = 2\pi/\omega)\rangle = \frac{\gamma\hbar}{2}A^2\exp[i\delta t + 2i\rho(t)] + \frac{\gamma\hbar}{2}C^2. \qquad [58]$$

We will assume below that $x \ll 1$ so that we can approximate $\rho(t)$ analytically using $\rho_1(t)$ from Section IIIC. In this limit, one can show that C^2 is of order x^2, and so the second term on the RHS of Eq. [58] is negligible compared to the first. Thus, for $x \ll 1$, which we will assume for the remainder of this section,

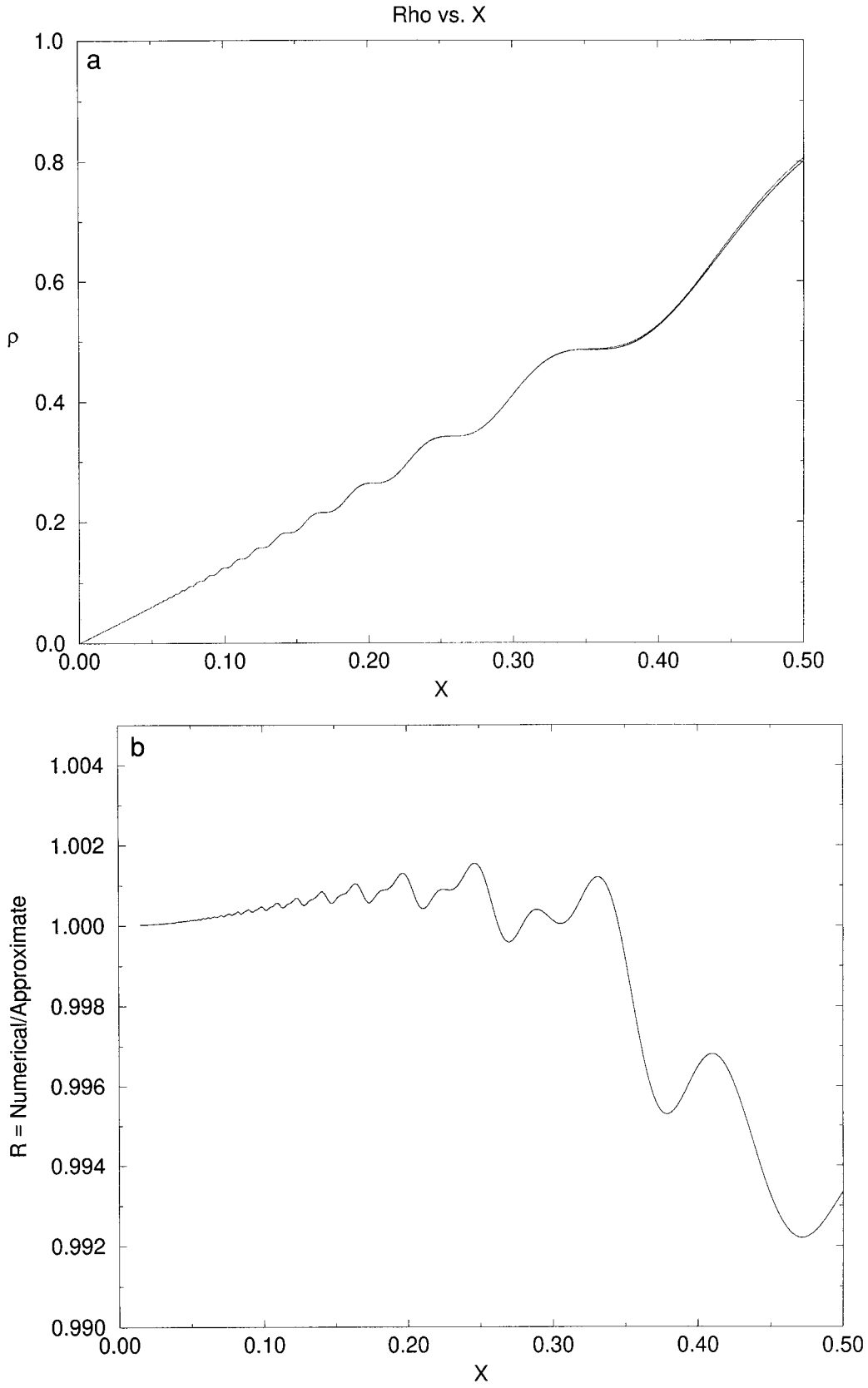

FIG. 3. (a) Plot of the non-adiabatic corrections to Berry's phase as a function of $x = \hbar\omega/2R$. The numerically determined exact result ρ and the first-order analytical approximation ρ_1 are plotted. The two curves overlap for x less than approximately 0.4, while for $x \geq 0.4$, the two curves begin to deviate slightly, with ρ_1 corresponding to the upper curve. (b) Comparison of the exact numerical result for the non-adiabatic corrections to Berry's phase ρ to the first-order analytical approximation ρ_1. The ratio ρ/ρ_1 is plotted versus $x = \hbar\omega/2R$.

$$\langle M_x(t = 2\pi n/\omega)\rangle = \frac{\gamma\hbar A^2}{2}\cos[\delta t + 2\rho_1(t)]. \quad [59]$$

Using Eqs. [51] and [45], Eq. [59] can be written as

$$\langle M_x(t = 2\pi n/\omega)\rangle = \frac{\gamma\hbar A^2}{2}\cos[\Omega_0 t + \beta \sin \Omega_0 t], \quad [60]$$

where

$$\beta = 2a(x), \quad [61]$$

and $a(x)$ is given in Eq. [52]. We see that the NMR signal has become frequency modulated by the oscillations in $\rho_1(t)$: the carrier frequency is Ω_0, and the amplitude β of the modulating signal is small since $x \ll 1$.

To explicitly display the consequences of this frequency modulation, we rewrite Eq. [60] as

$$\langle M_x(t = 2\pi n/\omega)\rangle = \mathrm{Re}[A_c \exp(i\Omega_0 t)\exp(i\beta \sin \Omega_0 t)], \quad [62]$$

where $A_c = \gamma\hbar A^2/2$. The second exponential factor on the RHS of Eq. [62] is periodic with period $T_m = 2\pi/\Omega_0$. Thus, it can be expanded in a Fourier series,

$$\exp[i\beta \sin \Omega_0 t] = \sum_{n=-\infty}^{\infty} c_n \exp[in\Omega_0 t], \quad [63]$$

with

$$c_n = \frac{1}{T_m}\int_{-T_m/2}^{T_m/2} dt\, \exp[i(\beta \sin \Omega_0 t - n\Omega_0 t)]$$
$$= \frac{1}{2\pi}\int_{-\pi}^{\pi} du\, \exp[i(\beta \sin u - nu)] = J_n(\beta). \quad [64]$$

In the last step we have used a well-known integral representation for the Bessel function $J_n(\beta)$ (*6*). Using Eq. [64] in Eq. [62] gives

$$\langle M_x(t = 2\pi n/\omega)\rangle = \sum_{-\infty}^{\infty} A_c J_n(\beta)\cos[t(\Omega_0 + n\Omega_0)]. \quad [65]$$

We see that frequency modulation has introduced all the harmonics of Ω_0 into the NMR signal. Since $\beta \ll 1$ when $x \ll 1$, we have that (*7*)

$$J_n(\beta) \approx \frac{\beta^n}{2^n n!} \quad (0 \le \beta \ll 1). \quad [66]$$

Thus, we only need to keep $n = 0, \pm 1$ in Eq. [65] so that

$$\langle M_x(t = 2\pi n/\omega)\rangle = \frac{\gamma\hbar A^2}{2}\left[\cos \Omega_0 t - \frac{\beta}{2}(1 - \cos 2\Omega_0 t)\right]. \quad [67]$$

We see that, when $x \ll 1$, frequency modulation produces a weak DC-component, and a weak second harmonic of Ω_0 in the NMR signal. The carrier frequency Ω_0 gives the NMR resonance frequency, which, for $x \ll 1$, is

$$\Omega_0 = \frac{2R}{\hbar}\left[1 - x\cos\theta + \left(\frac{x^2}{2}\sin^2\theta + \frac{x^3}{2}\sin^2\theta\cos\theta\right) + \mathbb{O}(x^4)\right]. \quad [68]$$

The experiment of Suter *et al.* (*5*) observed the first two terms on the RHS of Eq. [68]: here the second term is the resonance frequency shift produced by Berry's phase. The third term in Eq. [68] is the lowest order non-adiabatic correction to the resonance frequency, and is a consequence of ρ_0. A repetition of the the Suter *et al.* experiment would be very interesting, only this time focusing on whether the observed non-adiabatic resonance frequency corrections agree with those appearing in Eq. [68]. A search for the harmonics of Ω_0 in the NMR signal would also be very interesting.

IV. CLOSING REMARKS

In this paper we have presented a non-perturbative method for determining all non-adiabatic corrections to Berry's phase. The problem of determining these corrections has been reduced to solving an ordinary differential equation (ODE) for which numerical methods should provide solutions in a variety of situations.

We applied our method to a particular example which can be realized as an NMR experiment, and whose Schrödinger equation can be solved exactly. For this example, our method could also be implemented exactly, and we saw that it yielded non-adiabatic corrections which were identical to those obtained from the exact solution. The exact non-adiabatic corrections to Berry's phase were evaluated numerically, and an analytical approximation scheme was developed which could be applied in the limit of weak non-adiabaticity. The non-adiabatic corrections obtained in the lowest order approximation were identical to those found by Berry (*3*), and by Datta *et al.* (*4*). At the next order of approximation, the non-adiabatic corrections were seen to contain an oscillatory component not present in

the lowest order approximation. These oscillations were clearly visible in the exact numerical results, and were shown to produce a frequency modulation of the NMR signal. The non-adiabatic corrections were also seen to cause a shift in the NMR resonance frequency.

We close with some final comments. (1) We stress the fact that our method is non-perturbative. The object determined by the previously mentioned ODE contains non-adiabatic corrections to all orders in the non-adiabatic coupling. (2) The phase we determine is different from the Aharonov–Anandan phase (*8*). In the scenario that we consider, it is the system Hamiltonian which executes a cyclic evolution. Because the time dependence is non-adiabatic, the quantum system does not return to its initial state at the end of a cycle of the Hamiltonian, and so its state will not, in general, execute a cyclic evolution. The phase we have evaluated is, in fact, the Pancharatnam phase (*9–11*), and we have explicitly seen that it reduces to Berry's phase in the limit where the non-adiabaticity goes to zero. We have also seen, for the example considered in Section III, that no geometric phase appears in the transition amplitude (see Eq. [57]), in agreement with Berry (*12*) since $\phi(t)$ is an odd function of t in this case. (3) It would be interesting to apply the method presented here to the case of an environment undergoing non-adiabatic stochastic motion. As discussed in Ref. (*13*), the results of such an analysis will be relevant to an ongoing controversy connected with the motion of vortices in superconductors. The controversy centers on whether a certain Berry phase effect is masked by a secondary process connected with quasiparticle states bound to the vortex core. Activation of this secondary process requires a sufficiently large energy-level broadening of the bound states arising from finite temperature and/or impurity concentration. Reference (*13*) showed that Berry phase effects will produce energy-level broadening in the states of a two-level system coupled to an environment undergoing adiabatic stochastic motion. Because of the restriction to adiabatic stochastic motion, the energy-level broadening produced is too small to activate the secondary process in the vortex problem. A combination of the approach of Ref. (*13*) with that of the present paper produces a theoretical framework which can handle an environment undergoing non-adiabatic stochastic motion. This combined approach should allow us to determine whether Berry phase effects and non-adiabaticity can produce sufficient energy-level broadening to activate the above-mentioned secondary process. If so, one finds the interesting situation in which a Berry phase effect is masked by a secondary process whose activation is dependent upon Berry phase effects! We hope to report on this application in a future paper.

ACKNOWLEDGMENTS

It is a pleasure to thank Alan Bishop and the T-11 group at Los Alamos National Laboratory for the hospitality and support they provided during the time in which this work was done. I also thank T. Howell III for continued support.

REFERENCES

1. M. V. Berry, *Proc. R. Soc. London Ser. A* **392,** 45 (1984).
2. B. Simon, *Phys. Rev. Lett.* **51,** 2167 (1983).
3. M. V. Berry, *Proc. R. Soc. Lond. Ser. A* **414,** 31 (1987).
4. N. Datta, G. Ghosh, and M. H. Engineer, *Phys. Rev. A* **40,** 526 (1989).
5. D. Suter, G. C. Chingas, R. A. Harris, and A. Pines, *Mol. Phys.* **61,** 1327 (1987).
6. E. T. Whittaker and G. N. Watson, "A Course of Modern Analysis," p. 362, Cambridge Univ. Press, Cambridge, UK (1978).
7. See Ref. (*6*), p. 355.
8. Y. Aharonov and J. Anandan, *Phys. Rev. Lett.* **58,** 1593 (1987).
9. S. Pancharatnam, "Collected Works of S. Pancharatnam," Oxford Univ. Press, London (1975).
10. M. V. Berry, *J. Mod. Optics* **34,** 1401 (1987).
11. J. Samuel and R. Bhandari, *Phys. Rev. Lett.* **60,** 2339 (1988).
12. M. V. Berry, *Proc. R. Soc. London. Ser. A* **430,** 405 (1990).
13. F. Gaitan, *Phys. Rev. A* **58,** 1665 (1998).